

# Controlling the order of wedge filling transitions: the role of line tension

J. M. Moreno-Erriquez

Departamento de Física Atomica, Molecular y Nuclear, Área de Física Teórica,  
Universidad de Sevilla, Apartado de Correos 1065, 41080 Sevilla, Spain

A. O. Parry

Department of Mathematics, Imperial College 180 Queen's Gate, London SW7  
2AZ, United Kingdom

**Abstract.** We study filling phenomena in 3D wedge geometries paying particular attention to the role played by a line tension associated with the wedge bottom. Our study is based on transfer matrix analysis of an effective one dimensional model of 3D filling which accounts for the breather mode excitations of the interfacial height. The transition may be first-order or continuous (critical) depending on the strength of the line tension associated with the wedge bottom. Exact results are reported for the interfacial properties near filling with both short-ranged (contact) forces and also van der Waals interactions. For sufficiently short-ranged forces we show the lines of critical and first-order filling meet at a tricritical point. This contrasts with the case of dispersion forces for which the lines meet at a critical end-point. Our transfer matrix analysis is compared with generalized random-walk arguments based on a necklace model and is shown to be a thermodynamically consistent description of fluctuation effects at filling. Connections with the predictions of conformal invariance for droplet shapes in wedges is also made.

PACS numbers: 68.08.Bc, 05.70.Np, 68.35.Rh, 05.40.-a

## 1. Introduction

Fluid adsorption on micropatterned and sculpted solid substrates exhibit novel phase transitions compared to wetting behaviour at planar, homogeneous walls [1, 2, 3]. The simple 3D wedge geometry has been extensively studied in the past decade theoretically [4, 5, 6, 7, 8, 9, 10, 11, 12, 13, 14], experimentally [15, 3, 16, 17] and by computer simulation [18, 19, 20]. Thermodynamic arguments [21, 22, 23] show that the wedge is completely filled with liquid provided the contact angle is less than the tilt angle. These studies show that the conditions for continuous wedge filling transition are less restrictive than for critical wetting at planar walls [5, 6]. Close to critical filling, the substrate geometry enhances interfacial fluctuations, which become highly anisotropic. We refer to these as breather modes excitations [5, 6]. However, most of these studies neglect the presence of a line tension associated with the wedge bottom. Previous studies by the authors [13, 14] for short-ranged binding potentials show that the line tension may play an important role in filling phenomena and may drive the transition first-order if it exceeds a threshold value. We extend our analysis to arbitrary binding potentials, in particular to van der Waals dispersive interactions. Again, this shows that we can induce first-order filling by tailoring (micropatterning) the substrate close to the wedge bottom. This may provide a practical means of reducing the fluctuation effects which would otherwise dominate any continuous filling transition. This finding may have technological implications for microfluidic devices. However, the borderline between first-order and critical filling depends on the specific range of the interactions. If the binding potential between the interface and the wall decays faster than  $1=z^4$ , where  $z$  is the local interfacial height above the substrate, both regimes are separated by a tricritical point, as in the case of contact binding potentials [13, 14]. On the other hand, for longer-ranged binding potentials, a critical end point separates the first-order and critical filling transitions. We note that these two situations correspond exactly to the fluctuation-dominated and mean-field regimes for critical filling [5, 6].

Our Paper is arranged as follows: In Section II we review briefly the phenomenology of wedge filling and introduce the breather mode interfacial model used in our study. The definition of the path integral used in our transfer matrix analysis is discussed in some detail. While other formalisms have been forwarded they suffer from a number of problems. As we shall show our definition is consistent with thermodynamic requirements (exact sum-rules), generalized random walk arguments and also the predictions of conformal invariance. Section III is devoted to the analysis of wedge filling for contact binding potentials. Some of these results have been previously reported, without derivation, in a brief communication [13, 14]. Section IV extends the transfer matrix analysis to the important practical case of filling with long-ranged van der Waals forces. We conclude with a brief discussion and summary.

## 2. The model

Our starting point is the interfacial Hamiltonian pertinent to filling in shallow wedges (small tilt angle) [4]:

$$H = \int dxdy \left[ \frac{1}{2} (\nabla z)^2 + W(z) \right] \delta(\mathbf{r} \cdot \mathbf{n}) \quad (1)$$

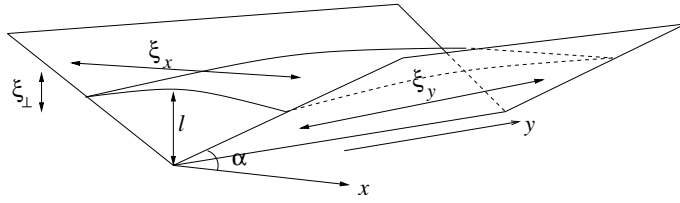


Figure 1. Schematic illustration of a typical interfacial configuration in the 3D wedge geometry. The diverging lengthscales at the filling transition are highlighted.

where  $z(x; y)$  is the local height of the liquid-vapour interface relative to the horizontal,  $\gamma$  is the liquid-vapour surface tension and  $W(z; x)$  is the binding potential between the liquid-vapour interface and the substrate (see figure 1). Hereafter we assume the temperature defines the energy scale and set  $k_B T = 1$ . To first approximation we may suppose that  $W(z; x)$  is independent of the position across the wedge section, i.e.  $W(z; x) = W(z)$ , where  $W(z)$  is the binding potential due to a single flat substrate. Corrections may arise when the liquid adsorption is small enough however – a point we shall return to later.

A mean-field analysis shows that locally the interface across the wedge is flat and that fluctuation effects are dominated by pseudo-one-dimensional local translations in the height of the filled region along the wedge (the breather modes) [5, 6]. Fluctuation effects at filling can be studied by using an effective pseudo-one-dimensional wedge Hamiltonian which accounts only for the breather-mode excitations [5, 6]:

$$H_W[l] = \frac{1}{2} \frac{d^2 l}{dy^2} + V_W(l) \quad (2)$$

where  $l(y) = z(0; y)$  is the local height of the interface above the wedge bottom. The effective bending term  $(l)$  resisting fluctuations along the wedge can be expressed as [5, 6]:

$$(l) = \frac{2}{2} + \frac{2}{2} \quad (3)$$

where  $\gamma$  is the line tension associated with the contact lines between the filled region and the substrate far from the wedge bottom. Note that for large  $l$ , we may neglect the contribution since  $(l)$  is proportional to the local interfacial height. Similarly, for large  $l$  the effective binding potential  $V_W(l)$  takes the form [5, 6]:

$$V_W(l) = \frac{h(l^2 - \frac{2}{2})}{2} + \frac{(l^2 - l^2)(l - l)}{(l - l)} + 2 + l^0 + \frac{1}{2} \frac{d^2 W(l - \frac{2}{2})}{dx^2} \quad (4)$$

The first two terms corresponds to the bulk and surface thermodynamic contributions required to form the filled liquid region [7]. Here  $h$  denotes the bulk ordering field measuring deviations from bulk two-phase coexistence,  $\gamma$  is the contact angle of the liquid drop at the planar wall-vapour interface and  $l^0$  is the equilibrium liquid layer thickness for a single planar wall. The line tension  $\gamma$  is defined as above, and  $l^0$  is the line tension associated with the wedge bottom. Note that the line tension contributions

are essentially independent of  $l$  for  $l \ll 1$ , so they become irrelevant in that limit. Finally, the last term corresponds to the binding potential contribution to  $V_W$ . Upon minimisation of  $V_W(l)$ , we recover the mean-field expression for the mid-point height (at bulk coexistence) [5, 6]:

$$\frac{2}{2} = W(l) + \frac{2}{2} W(l) \quad (5)$$

However, we stress that the form (4) for  $V_W(l)$  is only valid for  $l \ll 1$ . For  $l \gg 1$ , both  $W(l)$  and  $V_W(l)$  will behave in a different manner. Furthermore, we may control the adsorption properties for small  $l$  by micro patterning a stripe along the wedge bottom, so as to weaken the local wall-liquid intermolecular potential. The interfacial binding potential is consequently strengthened, and under some conditions it may bind the liquid-vapour interface to the wedge bottom even at the filling transition boundary  $l = 0$ . Thus by introducing a line tension associated with the wedge bottom one may induce first-order filling in the modified wedge provided the modification is strong enough. As we shall see the lines of first-order and continuous filling transitions are separated by either a tricritical point or a critical end point depending on the range of the intermolecular forces.

The quasi-one-dimensional character of the Hamiltonian means it is amenable to a transfer matrix analysis. The partition function corresponding to this Hamiltonian can be expressed as the following path integral [24]:

$$Z(l_b; l_a; Y) = \int Dl \exp(-H_W(l)) \quad (6)$$

However, the presence of a position-dependent stiffness coefficient makes the definition of the partition function ambiguous. This problem was pointed out, but not satisfactorily resolved, in [8] and is intimately related to issues associated with the canonical quantization of classical systems with a position-dependent mass [25, 26]. In this paper we use the following definition of the partition function:

$$Z(l_b; l_a; Y) = \lim_{N \rightarrow \infty} \frac{1}{N!} \int dl_1 \dots dl_{N-1} K(l_j; l_{j-1}; Y) \quad (7)$$

where  $l_0 = l_a$  and  $l_N = l_b$ , and  $K(l; l'; Y)$  is defined as:

$$K(l; l'; Y) = \frac{(-1)^{(l-l')^2}}{2^{\frac{p}{2}} Y^{\frac{p}{2}}} e^{-\frac{p}{2Y} (l-l')^2 - Y V_W(l)} \quad (8)$$

The partition function  $Z(l_b; l_a; Y)$  satisfies the differential equation

$$H_W Z(l_b; l_a; Y) = \frac{\partial Z(l_b; l_a; Y)}{\partial Y} \quad (9)$$

with initial condition  $Z(l_b; l_a; Y) = (l_b - l_a)$  as  $Y \rightarrow 0$ . The operator  $H_W$  is defined as [26]:

$$H_W = \frac{1}{2} \frac{\partial}{\partial l_b} - \frac{1}{(l_b) \partial l_b} + V_W(l_b) + V_W(l_b) \quad (10)$$

where  $V_W(l)$  is given by

$$V_W(l) = \frac{1}{2} \frac{l^2}{(l)} - \frac{3}{4} \frac{V^0(l)}{(l)}^2 - \frac{V^\infty(l)}{2(l)} \quad (11)$$

and prime denotes differentiation with respect to argument. The solution of (9) can be expressed via the spectral expansion [24]:

$$Z(l_b; l_a; Y) = \sum_{X} f_X(l_b) f_X(l_a) e^{-E_X Y} \quad (12)$$

where  $f_X(l)$  is a complete orthonormal set of eigenfunctions of the Hamiltonian operator  $H_W$ , with associated eigenvalues  $E_X$ .

Analogous to discussion of 2D wetting [24] we can now obtain the interfacial properties from the knowledge of the propagator  $Z(l_b; l_a; Y)$ . In particular, the probability distribution function (PDF),  $P_W(l)$ , can be obtained as:

$$P_W(l; Y) = \lim_{L \rightarrow 1} \frac{Z(l; l_{L=2}; Y + L=2) Z(l_{L=2}; l; L=2 - Y)}{Z(l_{L=2}; l_{L=2}; L)} \quad (13)$$

while the joint probability  $P_W^{(2)}(l_1; l_2; Y_1; Y_2)$  of finding the interface at midpoint heights  $l_1$  and  $l_2$  at positions  $Y_1$  and  $Y_2$  ( $> Y_1$ ), respectively, is:

$$P_W^{(2)}(l_1; l_2; Y_1; Y_2) = Z(l_2; l_1; Y_2 - Y_1) \lim_{L \rightarrow 1} \frac{Z(l_1; l_{L=2}; Y_1 + L=2) Z(l_{L=2}; l_2; L=2 - Y_2)}{Z(l_{L=2}; l_{L=2}; L)} \quad (14)$$

Further simplifications arises if we assume the existence of a bounded ground eigenstate  $0$ . Then, substitution of the spectral expansion (12) into (13) reads (for infinitely long wedge)

$$P_W(l) = j_0(l) \quad (15)$$

Similarly the excess wedge free-energy per unit length of an infinitely long wedge is identified with the ground eigenvalue  $E_0$ . The two-point correlation function  $h(l_1; l_2; Y)$  can be obtained in a similar manner:

$$h(l_1; l_2; Y) = \frac{P_W^{(2)}(l_1; l_2; 0; Y)}{P_W(l_1) P_W(l_2)} = \frac{(l_1)_0(l_1) (l_2)_0(l_2) \exp[-(E_1 - E_0)Y]}{\epsilon_0} \quad (16)$$

For large separations this vanishes exponentially allowing us to determine the correlation length  $\gamma = (E_1 - E_0)^{-1}$ , where  $E_1$  is eigenvalue corresponding to the first excited eigenstate. This result still holds even if  $E_1$  corresponds to the lower limit of the continuous part of the spectrum of  $H_W$ , although now the leading order of  $h(l_1; l_2; Y)$  is not purely exponential but is modulated by a power of  $Y$ .

An interesting connection with 2D wetting problems can now be seen. Introducing the change of variables [27]

$$Z(l) = \frac{P}{dl} \overline{(l)} \quad ; \quad (l) = (l)^{1/4} \quad (l(l)) \quad (17)$$

the eigenvalue problem  $H_W(l) = E(l)$  transforms to the following Schrodinger-like equation:

$$\frac{1}{2} \frac{d^2}{dl^2} (l) + V_W(l(l)) + \nabla_W(l(l)) (l) = E(l) (l) \quad (18)$$

where  $\nabla_W$  is defined as:

$$\nabla_W(l) = \frac{3}{32 l^2(l(l))} \frac{d(l(l))}{dl}^2 + \frac{1}{8 l(l(l))} \frac{d^2(l(l))}{dl^2} \quad (19)$$

(18) shows that the filling problem can be mapped onto a 2D wetting problem in the variable, under an effective binding potential. In our case  $(l) = 2 \frac{1}{l^p}$ , so we obtain  $V_W(l) = -3 = 16 l^3$ . The change of variables (17) leads to  $l = \frac{8}{8-9l^{3-2}}$  and thus  $V_W(l) = -5 = 72^2$ . Note that the use of the variable  $l / l^{3-2}$  as the appropriate collective coordinate has been previously recognized in the literature [8, 7]. However, our definition of the path integral (7) and (8) leads to a novel term in the wedge binding potential, which will be essential in our study and ensures thermodynamic consistency.

The filling potential  $V_W(l)$  must fulfill some requirements. In order that the interface does not penetrate the substrate,  $V_W(l)$  has a hard-wall repulsion for  $l < 0$ . Consequently we need to impose an appropriate boundary condition on the eigenfunctions of  $H_W$  at  $l = 0$ . The analytical expression of the boundary condition is obtained by a regularization procedure: we assume that the filling potential  $V_W$  and the position-dependent stiffness are constant for  $l < \epsilon_0$ , where  $\epsilon_0$  is some microscopic scale. Furthermore, we impose that  $V_W(l)$  must be continuous at  $l = \epsilon_0$ , so  $(l < \epsilon_0) = 2 \epsilon_0 = 0$ . On the other hand, the filling potential can take an arbitrary value  $U$ . The latter square-well potential models the modification of the filling potential  $V_W(l)$  for small due to the line tension associated with the wedge bottom. The eigenstates must fulfill the usual matching conditions that  $\psi$  and  $\psi' = \partial_l \psi$  are continuous at  $l = \epsilon_0$ . Finally, we consider the appropriate scaling limit as  $\epsilon_0 \rightarrow 0$ .

The qualitative form of the filling potential depends on the order of the mean-field phase transition [5, 6]. For critical filling with long-ranged intermolecular forces, the binding potential at bulk coexistence behaves as

$$V_W(l) = \frac{(-2 - 2)l}{(p-1)} + \frac{2A}{l^{1-p}} + \dots \quad (20)$$

where  $A$  is a Hamaker constant while the exponent  $p$  depends on the range of the forces. Specifically, for non-retarded van der Waals forces  $p = 2$ . For systems with short-ranged forces this is replaced by an exponential decay  $\exp(-l/\xi)$  where  $\xi$  is an inverse bulk correlation length. The presence of the fluctuation-induced filling potential  $V_W(l) / l^{1-3}$  in (9) gives rise to two distinct scenarios. For  $p > 4$  and large  $l$ , the direct contribution in  $(9) / l^{1-p}$  is negligible compared to the fluctuation-induced potential  $V_W$  arising from the position dependent stiffness. In this case we anticipate universal, fluctuation-dominated behaviour. On the other hand, for  $p < 4$  and large  $l$  we can neglect  $V_W$ . Since the  $l^{1-p}$  contribution to the binding potential is now repulsive, we expect a qualitatively different phase diagram. It is worthwhile noting that both situations exactly correspond to the existence of a mean-field and a filling fluctuation-dominated regimes for the filling transition predicted from heuristic arguments [5, 6].

We will consider two cases which correspond to different regimes of the filling transition. The contact interaction will be studied as the paradigm of the filling fluctuation-dominated regime. On the other hand, the van der Waals ( $p = 2$ ) case is analysed as a prototypical case of the mean-field regime.

### 3. Results for contact interactions

We consider first the case of short-ranged potentials. Some of our results have been reported in a brief communication but without detailed explanation [13, 14]. Here we provide full details of our transformatrix solution and present new results for the form

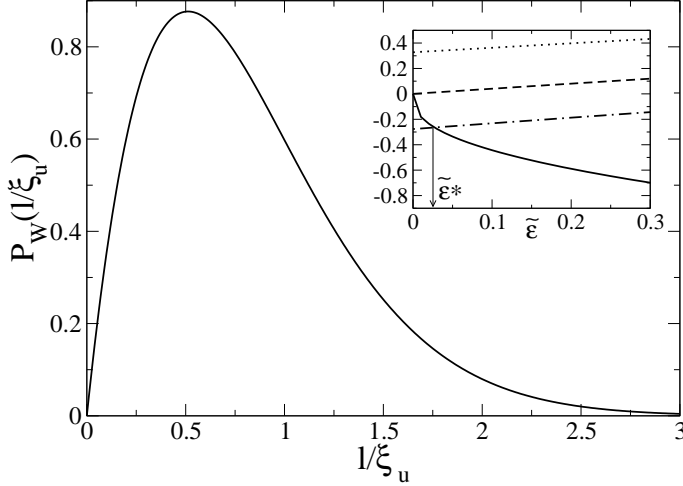


Figure 2. Scaled probability distribution function  $P_w(l/\xi_u)$  as a function of the scaled wedge midpoint interfacial height  $l/\xi_u$  for  $p=1$ . Inset: Plot of  $\sim \epsilon^3 A \Gamma(-\sim \epsilon^3) = A \sim \epsilon^3$  (continuous line) and  $\sim \epsilon^3 \sim \cot u \sim 1=2$  for  $u=0.5 < u_c$  (dotted line),  $u=u_c=1.358$  (dashed line) and  $u=2.0 > u_c$  (dot-dashed line). For the latter case, the value of the reduced ground eigenvalue  $\sim \epsilon^3$  is highlighted.

of the propagator. At lengthscales much larger than that of the bulk correlation length  $\xi_u$  we may write  $V_w(l) = (l^2 - l^2)l^2$  for  $l > 0$  and allow for line tension arising from the wedge bottom via a suitable boundary condition at the origin. Analysis of (9) shows that the short-distance behaviour of the eigenfunctions will be dominated by the  $l^{-3}$  contribution to the effective filling potential. In fact,  $\sim l^3$  or  $l^{3/2}$  as  $l \rightarrow 0$ , so the PDF function  $P_w(l; \sim l)$   $\sim l$  or  $\sim l^{1/2}$  as  $l \rightarrow 0$ . We anticipate that the latter behaviour corresponds to the critical filling transition as predicted by scaling arguments [7], but the former will be a completely new situation which, as we shall see, is related to the possibility of tricriticality. Turning to the critical filling transition first we note that the short-distance behaviour of the PDF,  $P_w(l; \sim l)$ , which emerges from our analysis, is indeed the required, thermodynamically consistent, result. This short-distance expansion ensures that the local density of matter near the wedge bottom contains a scaling contribution that vanishes  $\sim T - T_f$ , where  $T_f$  is the filling temperature. This is the required singularity which emerges from an analysis of sum-rules connecting the local density near the wedge bottom to (derivatives of) the excess wedge free-energy [28]. This leads us to conclude that our definition of the path integral in (8) is the correct one for the 3D wedge filling problem. As we shall see it also ensures that our model is conformally invariant.

### 3.1. Wedge filling along the $\sim l = 0$ path

At the filling phase boundary ( $\sim l = 0$ ), the problem can be mapped onto the intermediate fluctuation regime of 2D wetting [29] via (18). We apply the regularization method described above, and consider the scaling limit  $\sim l \rightarrow 0, U \rightarrow 1$

and  $4 U_0^3 = 1$ . Under these conditions, the ground eigenvalue  $E_0$  satisfies

$$\frac{p_u}{u} \sim \cot u \sim \frac{1}{2} = \frac{1}{3} \frac{Ai^0}{Ai} \sim 1/3 \quad (21)$$

where  $\sim = 4 E_0^3 = 1$  and  $Ai(x)$  is the Airy function. Graphical solution of (21) (see inset of figure 2) shows that there is a bound state with  $E_0 < 0$  for  $u > u_c$ , where  $u_c = 1.358$ . Otherwise  $E_0 = 0$  and there is no bound state. The existence of a bounded ground state at  $= 1$  implies that the filling transition is first-order for  $u > u_c$ , and critical for  $u < u_c$ . The explicit form of the PDF for  $u > u_c$  in the thermodynamic limit is

$$P_w(l; \beta) = \frac{6}{u} \frac{1}{u} \frac{1}{u} \frac{1}{u}^2 \quad (22)$$

where  $u = \beta = 1/3 / (u - u_c)$  as  $u \gg u_c$ . Note that the lengthscale  $u$  can be arbitrary large as  $u \gg u_c$ . Figure 2 plots the PDF in terms of the scaling variable  $l = u$ . For small  $l$ ,  $P_w(l; \beta) \sim l^u$ , with a short-distance exponent (SDE)  $u = 1$ . Asymptotically  $P_w(l; \beta) \sim \exp(-4(l/u)^{3/2} = 3)$  as  $l \gg 1$ .

The mean interfacial midpoint height  $l_w$ , height and roughness,  $\overline{h^2}$ , satisfy  $l_w = l_h = l_r$  showing that, in the scaling limit, there is only one lengthscale controlling the fluctuations of the interfacial height. Finally, the correlation length along the wedge axis  $y$  close to the filling transition can be obtained as  $\gamma = 1/E_0 = 4 u^3 / (u - u_c)^3$  since we can identify  $E_1 = 0$ .

These observations indicate the emergence of a new relevant field (in the renormalization group sense)  $t_u / (u - u_c)$ , in addition to  $t / t_c$  and the bulk ordering field  $h$ . Thus the conditions  $= 1$ ,  $u = u_c$  and  $h = 0$  correspond to a tricritical point which separates the lines of first-order and critical filling transitions. The excess wedge free energy density  $E_0$  vanishes as  $E_0 \sim u^2 \sim t_u^3$  as  $u$  tends to  $u_c$  from above. Critical exponents for the divergence of the characteristic lengthscales can be defined as the tricritical point is approached along the  $= 1$  path:

$$l_w \sim t_u^u; \quad l_h \sim t_u^u; \quad l_r \sim t_u^u \quad (23)$$

Our results show that  $l_w = l_h = l_r = 1$  and  $u = 3$ . Finally, the effective wedge wandering exponent  $w = u = u = 1/3$ , which coincides with its value for the critical filling transition [5, 6].

For  $u > u_c$  and  $= 1$ , the interface is unbounded in the thermodynamic limit. However, we can study the finite-size behaviour of the droplet shape when the interface is pinned very close to the wedge bottom at positions  $y = L/2$ . Making use of results presented in the Appendix, in particular (A 11) and (A 12), we find that the PDF at the tricritical ( $u = u_c$ ) and critical ( $u = u_c$ ) wedge filling transition are given by

$$P_w^{u=u_c, \beta=1}(l; \beta) = \frac{\frac{2}{3} l}{3^{1/3} (2=3)} \exp\left(-\frac{(L/l)^3}{9}\right) \quad (24)$$

$$P_w^{u=u_c, \beta=L}(l; \beta) = \frac{\frac{4}{3} l^3}{3^{5/3} (4=3)} \exp\left(-\frac{(L/l)^3}{9}\right) \quad (25)$$

where

$$L = \frac{16}{L} \frac{1}{1} \frac{2Y}{L} \frac{2}{L} \quad (26)$$

The typical droplet shape  $m$  may be characterized by the most-probable position  $l_{\text{mp}}(y)$  which follows from the relation  $\partial P_W^L(l_{\text{mp}}) = 0$ , or by the average shape  $l_{\text{av}}(y)$  via the definition  $l_{\text{av}} = \int_0^L dl P_W^L(l)$  [24]. In all cases we find that the typical droplet shape follows  $l = c$ , where  $c$  is a number which depends on the definition of the typical shape and whether the pinning is at critical or tricritical filling. Consequently, the droplet shape  $m$  must obey:

$$y^2 + \frac{4}{c^3} l^3 = \frac{L^2}{4} \quad (27)$$

Satisfyingly this shape is precisely that predicted by the requirement of conformal invariance which can be used to map a droplet pinned at just one end to one pinned at two points ( $y = L/2$ ) [30]. This gives further indication that the definition of the measure used in our transformatrix formulation is appropriate for the wedge geometry.

### 3.2. The necklace model

A simple model can be introduced to understand the filling properties of the wedge at  $\gamma = 0$ . This model is a generalization of the necklace model introduced for 2D wetting [31, 32]. The interface is pinned to the wedge bottom along segments of varying length but unbinds between them, forming liquid droplets. We associate with each vertex a weight  $v$  which is related to the point tension between a bound and unbound state. Following the analysis described in [31], we introduce the generating function:

$$G(z) = \sum_{L=0}^{\infty} z^L Z_L \quad (28)$$

where  $Z_L$  is the interfacial canonical partition function of a segment of length  $L$  (which we assume to be discretized) and  $z$  is an activity-like variable. The pure pinned (A) and unbound (B) states have generating functions:

$$G_A = \sum_{L=0}^{\infty} Z_L^A z^L = (sz)^L \quad (29)$$

$$G_B = \sum_{L=0}^{\infty} Z_L^B z^L = \frac{(wz)^L}{L} \quad (30)$$

where  $s = \exp(-u)$ , with  $u$  as an effective line tension in units of  $k_B T$ . On the other hand,  $w = \exp(-\phi_0)$ , where  $\phi_0$  is the excess free energy per unit length of a long liquid droplet on the wedge, which we can assume to be zero by shifting the energy origin. Finally,  $\gamma$  is the exponent characterizing the first return of the interface to the wedge bottom. This can be calculated from the  $u \rightarrow u_c$  limit corresponding to the completely filled regime. As shown in (A.13) and (A.15) in the Appendix,  $\gamma = 4/3$ . Now the complete generating function is:

$$G(z) = G_A + G_A v G_B v G_A + \dots = \frac{G_A(z)}{1 - v^2 G_A(z) G_B(z)} \quad (31)$$

Thus there will be a continuous phase transition at  $u_c$  defined as [31]:

$$u_c = \ln w (1 - v^2 G_c) \quad (32)$$

where  $G_c = \sum_{L=0}^{\infty} Z_L^B = w^L$ . Below  $u_c$ , the interface is completely unbound while it remains pinned for  $u > u_c$ . The singularities of the various interfacial properties close to  $u_c$  are characterized by critical exponents. In particular, the specific heat

critical exponent  $\zeta_w^u$  and the longitudinal correlation length critical exponent  $\zeta_y^u$  can be expressed in terms of the exponent  $\zeta$  as [31, 32]

$$2 \zeta_w^u = \zeta_y^u = \frac{1}{1 - \zeta} \quad (33)$$

Substituting  $\zeta = 4/3$  we find the correct values  $2 \zeta_w^u = \zeta_y^u = 3$  derived earlier. In order to estimate the interfacial average height and roughness, we need the interfacial height PDF in a liquid bubble, which is given by (25). A similar argument to the one presented in [31] leads to:

$$\zeta_w^u = \frac{\overline{Y_B^{4-3}}}{\overline{Y_B}} ; \quad \zeta_y^u = \frac{\overline{Y_B^{7-3}}}{\overline{Y_B^2}} \quad (34)$$

where  $\overline{Y_B}$  is the length of a liquid bubble, and  $\overline{a}$  is the average of  $a$  in the pure liquid (B) phase. It is straightforward to see that  $\zeta_w^u = \zeta_y^u = 1$ , with  $\zeta = 1/3$ . Consequently,  $\zeta_w^u = \zeta_y^u = 1$ , in agreement with our exact results. Note that in contrast to the 2D wetting case [31, 32] the exponent associated to the probability of first return  $\zeta \neq 2 \zeta_w^u$ . This can be traced to the role played by the position dependent stiffness in the filling model (2) which biases the random-walk-like motion of the interface. As pointed out previously [14] it is remarkable that the critical exponents for 3D critical and tricritical wedge filling are identical to those anticipated for 2D complete and critical wetting with random bond disorder. The necklace model provides an elegant means of understanding this unusual dimensional reduction.

### 3.3. Wedge filling for $\zeta > 1$

Now we extend some of our previous results to partial filling conditions, i.e.  $\zeta > 1$ . The rescaling  $\zeta = (\zeta - 1)^{1/4} (2 - \zeta)^{3/8} = \frac{1}{2}$ ,  $\zeta = (\zeta - 1)^{1/2} (2 - \zeta)^{3/4} E$  transforms the Schrödinger equation (18) into a parameter free form

$$\frac{1}{4} \frac{d^2}{d\zeta^2} (\zeta) + \frac{3\zeta}{2} \frac{2-3}{2} \frac{5}{144\zeta^2} (\zeta) = (\zeta) \quad (35)$$

This leads directly to the critical behaviour of the mean mid-point height  $\zeta_w^u$  and the correlation length along the wedge  $\zeta_y^u$ , provided that the PDF is not singular, i.e. takes non-negligible values at finite values of  $\zeta$ . The PDF is obtained analogous to the case  $\zeta = 1$  case described above, from determination of the ground eigenstate  $\psi_0$ . We find for the PDF

$$P_w(\zeta; \zeta > 1) = C \frac{1}{2} \exp \left[ -\frac{1}{2} \left( \frac{\zeta}{\zeta_w^u} - \frac{1}{\zeta_y^u} \right)^2 \right] \quad (36)$$

where  $\zeta_w^u = 1/2$ ,  $\zeta_y^u = 1/2$ ,  $C = 1/\sqrt{2\pi}$  is the reduced ground eigenvalue,  $C$  is a normalization factor and  $H_s(z)$  is the s-order Hermite function [33]. As  $\zeta \rightarrow 0$ , the PDF vanishes (in general) like  $P_w(\zeta; \zeta > 1) \sim 1/\zeta$  while at large distances  $P_w(\zeta; \zeta > 1) \sim \exp[-2\zeta/\zeta_w^u]$  as  $\zeta \rightarrow \infty$ .

The value of the reduced ground eigenvalue  $\zeta_w^u$  depends on the boundary condition at  $\zeta = 0$ . In order to do this consistently we once again turn to a regularization

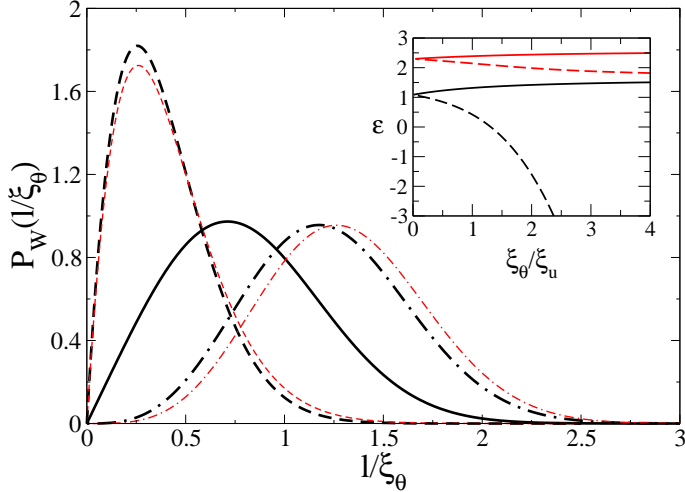


Figure 3. Plot of the scaled PDF for  $\xi_0 = 1.5$  (thick dashed line),  $\xi_0 = u_c$  (thick continuous line) and  $\xi_0 = 1.639$ , corresponding to  $u = u_c$  (thick dot-dashed line). For comparison, the PDF from (22) with  $u = 1.968$  (which corresponds to  $\xi_0 = 1.5$ , see inset) is also plotted (thin dashed line). Finally, the scaled PDF obtained in [8] is also shown (thin dot-dashed line). Inset: Plot of the ground (black lines) and first-excited (red lines) reduced eigenvalues  $E^3$  of  $H_w$  as a function of  $l/\xi_0$  for  $u < u_c$  (continuous lines) and  $u > u_c$  (dashed lines).

procedure: in the scaling limit ( $\xi_0 \rightarrow 0$  and  $4 \leq \xi_0^3 = u$ ), the reduced eigenvalues are the solutions of the equation:

$$\frac{1}{\xi_0} \frac{p_u}{u} \cot \frac{p_u}{u} \frac{1}{2} = + \frac{p^2}{2} \frac{p}{2} \frac{H \frac{2}{4} \frac{3}{2} \frac{p}{2}}{H \frac{2}{4} \frac{1}{2} \frac{p}{2}} \quad (37)$$

where  $\xi_0$  is the minimum value of them. For  $u$  close to  $u_c$ , we can expand the left-hand side of (37) around  $u_c$  as:

$$\frac{1}{\xi_0} \frac{p_u}{u} \cot \frac{p_u}{u} \frac{1}{2} \approx \frac{\frac{1}{3} \frac{3}{2} \frac{2}{3}}{\frac{1}{3} u} \quad (38)$$

where the positive (negative) sign corresponds to  $u > u_c$  ( $u < u_c$ ), respectively. This expression allows us to identify  $u_c / \xi_0 = j_1 u_c$  in a manner completely consistent with our expression obtained for  $u > u_c$  at  $\xi_0 = 0$ .

We obtain scaling behaviour for the wedge excess free-energy per unit length  $E_0$  (see also inset of figure 3):

$$E_0 = \frac{1}{3} \xi_0 \frac{1}{u} \left( \frac{u}{u_c} \right)^{\frac{2}{3}} \quad (39)$$

where  $c$  is an unimportant metric factor, and the sign corresponds to the situations  $u > u_c$  and  $u < u_c$  as above. The scaling two functions  $\xi_0^+$  and  $\xi_0^-$  have the following properties:

$$\xi_0^+(0) = \xi_0^-(0) = 1.086 \quad (40)$$

$$\xi_0^+(x) = \xi_0^-(x) \quad (41)$$

$$\xi_0^+(x) = 1.639 \quad (42)$$

The asymptotic behaviour of the PDF as the filling transition is approached, i.e.  $u \rightarrow u_c$ , is different for three situations: (i)  $u > u_c$ , (ii)  $u < u_c$  and (iii)  $u = u_c$  (see figure 3). For the case (i), saddle-point asymptotic techniques [34] applied to the PDF (36) recover the expression for the PDF (22). Consequently, the lengthscale governing the interfacial height and range of the breather mode fluctuations is  $u$ , which remains finite as  $u \rightarrow u_c$ . Thus on lengthscales compared to  $u$ , the PDF becomes a highly localized delta function located at  $l = 0.0$ . On the other hand, the first-excited eigenvalue scales as  $E_1 \sim u^{-3}$  (see inset of figure 3), so the lateral correlation length also remains finite,  $\gamma \sim u^{-3}$ .

For case (ii) we must take the limit (42) of the scaling function  $\phi$ . Substitution into (36) leads to the asymptotic behaviour of the PDF as  $u \rightarrow u_c$ . Now, the lengthscale which controls both the mean interfacial height and roughness is  $u$ . It is also interesting to note that  $P_W(1) \rightarrow 1$  for  $1 \rightarrow 0$ , so thermodynamic consistency is assured. Our solution is different from the PDF reported in [8, 7] (see figure 3) although the global behaviour is qualitatively similar. On the other hand, the lateral correlation length  $\gamma$  has the asymptotic behaviour  $\gamma = (E_1 - E_0)^{-1/3}$ .

Finally, the PDF for case (iii) is obtained by substitution of the limiting value (40) for  $\phi$  into (36). Although the relevant lengthscales behave asymptotically as in the case (ii), the scaled PDF is different, as shown in figure 3. In particular,  $P_W(1) \rightarrow 1$  as  $1 \rightarrow 0$ .

We can determine the critical exponents for fixed  $u$  as:

$$E_0 \sim t^w; l_w \sim t^w; \gamma \sim t^z; \gamma \sim t^y \quad (43)$$

where we define  $t = l_w / \gamma$ . For both critical and tricritical filling, our analysis shows that the critical exponents take the values  $w = 3/4$ ,  $z = 1/4$  and  $y = 3/4$ , so the wandering exponent is  $w = z = y = 1/3$ . These findings are in agreement with scaling predictions [5, 6]. Finally, we note that the tricritical gap exponent  $\alpha$ , which relates the critical exponents along the  $u = 0$  and  $u = \infty$  paths, can be obtained from the scaling form of  $E_0$  (39) as  $\alpha = 4$  [14].

#### 4. Results for dispersion forces

Wedge filling in systems with short-ranged forces is representative of the universality class of fluctuation dominated behaviour occurring if the exponent in the binding potential  $p > 4$ . In almost all practical realizations of wedge filling however, long-ranged, van der Waals forces from the liquid-liquid and solid-liquid intermolecular potentials will be present. While exceptions to this may be found, for example in polymer systems, the case of long-ranged forces is much more the rule than the exception. We wish to understand how such long-ranged forces alter the nature of the phase diagram and in particular the change from first-order to continuous filling behaviour. We can allow for the presence of long-ranged forces through the binding potential (20). For the three-dimensional case and non-retarded van der Waals interactions the value of  $p = 2$ . While higher order terms are present these will not play a significant role in determining the physics and can be safely ignored. Here we show that the potential

$$V_W(1) = \frac{(-2 + 2)l}{1} + \frac{2A}{l} \quad (44)$$

is amenable to exact analysis. The form of the total effective binding potential  $V_W(1) + V_W(l)$  is shown in figure 4. As one can see there is a local maximum for

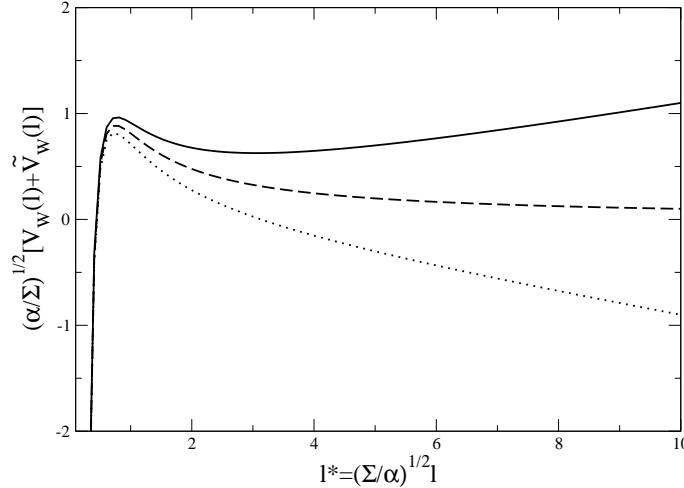


Figure 4. The effective wedge binding potential  $V_w(l) + \tilde{V}_w(l)$  for an effective Hamaker constant  $2A = 1$  and: (i)  $\epsilon^2 = 0.1$  (continuous line), (ii)  $\epsilon^2 = 0.01$  (dashed line) and (iii)  $\epsilon^2 = 0.001$  (dot-dashed line).

small which arises from the competition between the fluctuation-induced component and the van der Waals contribution. A rough estimate for its location can be obtained by setting  $\epsilon = 0$ , and a simple calculation leads to

$$l^* = \frac{3}{4} \frac{p}{2A} \quad (45)$$

For  $\epsilon > 0$ , a local minimum is obtained for larger  $l^*$ . This minimum arises from the balance between the thermodynamic contribution  $(\epsilon^2 - 1)^2$  and the van der Waals component of the effective binding potential. The position of the minimum is governed for  $\epsilon > 0$  by the mean-field interfacial height:

$$l_w^{MF} = \frac{2A}{(\epsilon^2 - 1)^2} \quad (46)$$

Since for long-ranged forces we anticipate that mean-field theory describes correctly the critical filling transition, a third lengthscale is the mean-field roughness, identified as [5, 6]:

$$l_w^{MF} = \frac{p}{2} \left( l_w^{MF} \right)^0 \left( \frac{M}{W} \right)^{1/4} \quad (47)$$

Since in our case  $W(l) = A = \frac{p}{2}$ , we find, from (46)

$$l_w^{MF} = \frac{p}{2} \quad (48)$$

where our definition of  $l^*$  is unchanged from the previous Section. It is remarkable that the roughness is independent of the strength of van der Waals interactions.

The fluctuation-induced contribution to the wedge binding potential suggests it may be possible to find a bound state at a lengthscale determined by  $l^*$ , for  $\epsilon > 0$ . However no bound state is possible for  $\epsilon < 0$ : any interface would tunnel through the barrier and unbind completely from the wedge bottom.

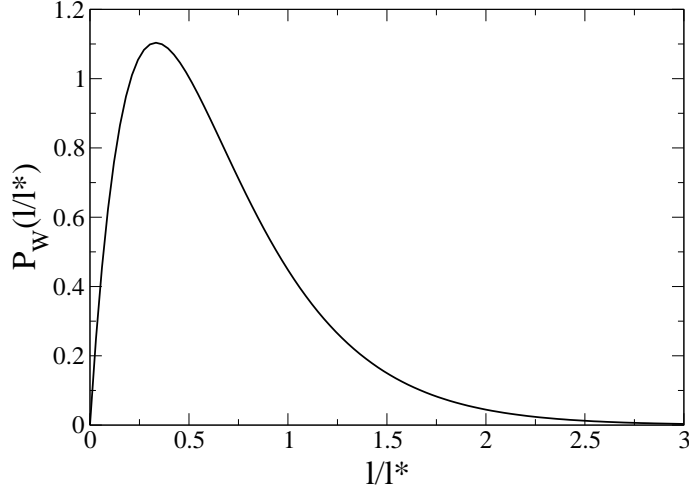


Figure 5. Scaled probability distribution function  $P_W(l/l^*)$  for  $l = l^*$  and  $u \neq u_c$  in presence of dispersion forces.

Our analysis proceeds along the same lines as the previous Section. First we investigate allowed states that exist at the filling phase boundary  $u = u_c$ , and then extend our analysis to the partial filling regime  $u > u_c$ .

#### 4.1. W edge filling along the $u = u_c$ path

First we suppose  $u = u_c$  and search for a bound state  $\psi_0(l)$  of  $H_W$ . As anticipated this is only possible if  $E_0 < 0$ , in which case the eigenfunction is given by

$$\psi_0(l) \propto \frac{1}{l} \text{Ai} \left( \frac{l}{u} \right) + \frac{9 \frac{u^2}{l}}{4(l)^2} \quad (49)$$

where we define as previously  $u_c = (4|E_0|)^{1/3}$ .

In order to obtain  $E_0$ , we make use of the regularization procedure. In the scaling limit this satisfies the equation:

$$\frac{1}{u} \sim \frac{1}{\cot u} \sim \frac{1}{2} = \frac{\text{Ai}^0 \sim^{1/3} + \frac{9 \frac{u^2}{l}}{4(l)^2}}{\text{Ai} \sim^{1/3} + \frac{9 \frac{u^2}{l}}{4(l)^2}} \quad (50)$$

where  $\sim = (u_c/u)^{1/3}$ . For values of  $\sim$  not too close to zero,  $u \rightarrow 0$  in the scaling limit, so the second term in the Airy function argument can be neglected. Thus the solution for  $\sim$  coincides with that corresponding to a contact binding potential. However, as  $\sim \neq 0$ , a crossover to a different situation is observed. In particular, for  $u \ll 1$  we can make use of the asymptotic expansion of the Airy function for large arguments:

$$\text{Ai}(x) \sim \frac{\exp(-\frac{2x^{3/2}}{3})}{2x^{1/4}} \quad x \neq 0 \quad (51)$$

Substituting into (50), we find that

$$\frac{1}{u} \sim \frac{1}{\cot u} \sim \frac{1}{2} = \frac{3}{21} \sim \frac{1}{3} \sim \frac{1 + 3}{3} \quad (52)$$

Next we define  $u_c$  as the value of  $u$  at which  $\sim = 0$ . It is straightforward to see that  $u_c = 1.358 + O(\epsilon_0=1)$ , so in the scaling limit the threshold for the existence of a bound state is the same as for the contact binding potential. Now we expand (52) for  $u$  around  $u_c$  and  $\sim$  around zero. In the scaling limit, we obtain that:

$$\sim \frac{u^2}{(1-\epsilon)^2} (u - u_c) \quad (53)$$

Finally, the PDF in this regime can be obtained from substitution of the asymptotic relationship (51) into (49). After some algebra, the PDF reads:

$$P_W(l) = \frac{91}{(1-\epsilon)^2} \exp\left(-\frac{31}{l}\right) \quad (54)$$

(see also figure 5). Since  $l$  remains finite at  $u_c$ , the interface remains bound as  $u$  approaches  $u_c$  from above, and suddenly unbinds for  $u > u_c$ . This identifies the point  $h = 0$ ,  $\sim = 0$  and  $u = u_c$  as a critical end point in the surface phase diagram. However, although  $u$  is not a relevant field in the renormalization-group sense, the longitudinal correlation length  $\zeta = F_0 j^{-1}$  diverges as  $(u - u_c)^{-1}$ . A similar behaviour occurs within the subregion C of the intermediate fluctuation regime for 2D wetting transitions [29].

#### 4.2. Wedge filling for $\epsilon > 0$

We now extend our results to  $\epsilon > 0$  proceeding in the same way we did for contact interactions. Again we can analytically obtain the ground state  $\phi_0(l)$  of  $H_W$  as:

$$\phi_0(l) / \frac{P_0}{l} \exp\left(-\frac{1}{l}\right) = \phi_0 - \frac{1}{H} \frac{\frac{2}{3} \frac{1}{2} \frac{9}{16} \frac{2}{(1-\epsilon)^2}}{\frac{1}{3} \frac{1}{2} \frac{9}{16} \frac{2}{(1-\epsilon)^2}} \frac{P_0}{2} \frac{1}{l} \frac{P_0}{2} \quad (55)$$

where  $\phi_0$ ,  $P_0$  and  $H_s(x)$  are defined as in (36) for the contact binding potential. Note that the dependence on the dispersion forces only appears at the orders of the  $H$ ermite function  $H_s$ .

The regularization procedure leads to the following equation for the reduced eigenvalues (for  $u$  close to  $u_c$ ):

$$\begin{aligned} -\frac{P_0}{u} \frac{u}{\cot u} \frac{P_0}{u} \frac{1}{2} - \frac{\frac{1}{3} \frac{3}{2} \frac{2}{3}}{\frac{1}{3} \frac{1}{2} \frac{9}{16} \frac{2}{(1-\epsilon)^2}} \frac{P_0}{2} = \\ + \frac{P_0^2}{2} \frac{P_0}{2} \frac{9}{4} \frac{2}{(1-\epsilon)^2} \frac{H}{H} \frac{\frac{2}{4} \frac{3}{2} \frac{9}{16} \frac{2}{(1-\epsilon)^2}}{\frac{2}{4} \frac{1}{2} \frac{9}{16} \frac{2}{(1-\epsilon)^2}} \frac{P_0}{2} \end{aligned} \quad (56)$$

and  $\phi_0$  is the minimum of the solutions. We can see that  $\phi_0$  will depend now not only on the ratio  $\epsilon = u_c$  and the sign of  $u - u_c$ , but also on  $\epsilon = 1$ . Nevertheless as for the case with a contact binding potential, we are mainly interested in the limit  $\epsilon \rightarrow 0$ , so that the lengthscale  $\zeta$  is very large.

For  $u > u_c$ , saddle-point asymptotic techniques analogous to those applied in the previous Section [34] show that the ground state of  $H_W$  converges to the expression (49) as  $\epsilon \rightarrow 0$ . Consequently we recover the results obtained earlier for the special case  $\epsilon = 0$ . This indicates that, for these values of  $u$ , the wedge filling transition must be first-order.

For  $u < u_c$  the non-existence of ground state for  $\epsilon = 0$  indicates that the filling transition is critical. We anticipate that mean-field theory will describe faithfully

singularities at the critical wedge filling [5, 6]. Thus we expect that the interfacial height PDF is centered around  $\frac{M}{W}^F$  with Gaussian fluctuations on the scale of  $\frac{M}{W}^F$  representing the breather mode excitations. The mean-field value of the excess free energy per unit length is given by  $V_W(\frac{M}{W}^F)$ . Consequently, the mean-field value of the reduced ground eigenvalue  $\frac{M}{0}^F$  is:

$$\frac{M}{0}^F = \frac{3}{21} \quad (57)$$

The shift of  $\frac{M}{0}^F$  with respect to  $\frac{M}{0}^F$  due to breather-mode fluctuations  $\frac{M}{0}$  can be estimated in the following way. We expand  $V_W$  around its minimum up to quadratic order, so the shift may be estimated via:

$$E_0 = \frac{1}{2} V_W^{(0)}(\frac{M}{W}^F) (\frac{M}{0}^F)^2 \quad (58)$$

implying that

$$\frac{M}{0}^F = \frac{1}{\frac{M}{0}^F} - \frac{1}{2} \quad (59)$$

which vanishes as  $\frac{M}{0}^F \rightarrow 0$ .

We can now proceed with a more formal derivation. Equation (55) can be written as:

$$P_0(l) / \frac{p}{2} \exp(-x^2/2) H_s(x) \quad (60)$$

where we have defined:

$$x = \frac{\frac{p}{2} \frac{1}{2}}{\frac{p}{2} \frac{0}{2}} \quad (61)$$

$$s = \frac{\frac{M}{0}^F}{2} \frac{0}{2} + \frac{(\frac{M}{0}^F)^2}{4} \quad (62)$$

with  $\frac{1}{2} \frac{p}{2} \frac{1}{2}$  and  $\frac{0}{2} = \frac{0}{0} \frac{M}{0}^F$ . Note that (60) is the wavefunction of the harmonic oscillator in the  $x$  coordinate (in units of  $\sim m^1$ ), modulated by the factor  $\frac{p}{2}$ . As in the latter case,  $\frac{0}{2}$  will increase exponentially as  $x \rightarrow 1$ , i.e.  $1 \rightarrow 0$  and large  $\frac{M}{0}^F$ , unless  $s$  is a non-negative integer. This result is independent of the explicit value of  $s = u$ . Consequently, the shift for the lowest eigenvalues is given by:

$$s = \frac{1}{(\frac{M}{0}^F)^2 + 4} n + \frac{1}{2} \frac{M}{0}^F - \frac{2n + 1}{\frac{M}{0}^F} \quad (63)$$

with  $n$  a non-negative integer. The ground eigenstate will correspond to the case  $n = 0$ . The corresponding PDF becomes a Gaussian:

$$P_W(l) = \frac{2}{\sqrt{2\pi}} \exp\left(-\frac{(l - hli)^2}{2}\right) \quad (64)$$

with  $hli = \frac{M}{W}^F + 21 = 3 \frac{M}{W}^F$ , and roughness  $\zeta = -2$ . Finally, the longitudinal correlation length  $\zeta = (E_1 - E_0)^{-1} = 3 \frac{M}{0}^F = 2 \left(\frac{M}{W}^F\right)^2$ .

Consequently, the explicit transfer matrix solution is in complete agreement with the predicted mean-field values for the critical exponents when  $p = 2$  [5, 6]:  $\zeta_w = 1=2$ ,  $\zeta_w = 1=2$ ,  $\zeta_y = 1$  and  $\zeta_z = 1=4$ .

## 5. Discussion and conclusions

In this paper we have reported analytical results for 3D wedge filling transitions in the presence of short-ranged and long-ranged (van der Waals) interactions based on exact solution of the continuum transfer equations for a pseudo one-dimensional interfacial Hamiltonian. First-order and continuous (critical) filling are possible for both types of force depending on the strength of the line tension associated with the decoration of the wedge bottom. Our analytical solution for the interfacial height PDFs at critical filling recovers the known values of the critical exponents for critical filling for short and long-ranged forces. In addition we have elucidated the nature of the cross-over from first to critical filling which occurs at a specific value of the wedge bottom line tension. This is qualitatively different for systems with short and long ranged forces whose surface phase diagrams are shown to have tricritical and critical end-points respectively. To finish we argue that these results, which are proto-typical of the fluctuation dominated and mean-field regimes respectively, are qualitatively valid for any type of binding potential. As already mentioned, the 3D wedge filling phenomenon can be mapped onto a 2D wetting problem with a new collective coordinate  $/ \tilde{l}^{=2}$ . If we suppose that, at the filling phase boundary,  $\tilde{l}^3 V_W(l) \rightarrow 0$  for large  $l$ , we can make use of a renormalization-group arguments to determine the allowed behaviour. As  $h$  and  $t / \tilde{l}^{=2}$  are always relevant operators, we will restrict ourselves to the filling transition boundary  $= 0$ ,  $h = 0$ . The effective 2D wetting binding potential decays faster than  $1/l^{=2}$ , so it becomes irrelevant in the renormalization-group sense [35, 36]. The renormalization-group flows are dominated by the unstable fixed point and the stable fixed point for the 2D wetting binding potential  $5=72^{=2}$ , which correspond to the tricritical and critical filling transition, respectively. Thus, for large scales the only effect of such binding potentials that decay faster than  $1/l^{=3}$  is to renormalize the line tension associated with the wedge bottom.

For long-ranged binding potentials i.e. those for which, at  $= 0$ ,  $\tilde{l}^3 V_W(l) \neq 0$  for large  $l$ , we may resort to a mean-field analysis [5, 6]. We expect that close to the filling transition the PDF is asymptotically a Gaussian characterized by the mean-field interfacial height  $\tilde{l}_W^{MF}$  and roughness  $\tilde{h}_W^{MF}$ . However, if the next-to-leading order to the wedge binding potential is determined by the short-distance repulsive part of  $W(z)$ , we find a similar scenario to the one depicted in figure 4. In particular, it is possible to bind the interface to the wedge bottom. The interfacial roughness will be controlled by the (microscopic) lengthscale  $l = 1$  corresponding to the maximum of the total effective binding potential. The existence of such a bound state, as well as the threshold to the critical filling transition will depend on the specific details of the interfacial binding potential.

The predicted filling phenomenology presented in this paper can hopefully be checked experimentally or by computer simulations of more microscopic models. Of course our predictions for contact (strictly short-ranged) forces requires the elimination of van der Waals forces which are ubiquitous for simple liquids. Here our results are most easily tested using large scale Ising model simulations. In this case it should be straightforward to induce first-order filling by weakening the local spin-substrate interaction near the wedge bottom. In contrast our predictions for first-order filling with van der Waals forces may well be amenable to experimental verification some time in the near future. Taking an even broader perspective it may be that the chemical decoration of a wedge bottom will provide a practical means of eliminating large scale interfacial fluctuations. This may be of relevance to the construction of microfluidic

devices whose efficiency will depend crucially on the control of fluctuation effects.

#### Acknowledgments

J.M.R.-E. acknowledges partial financial support from Secretaría de Estado de Educación y Universidades (Spain), co-financed by the European Social Fund, and from the European Commission under Contract MEIF-CT-2003-501042. A 'Ramón y Cajal' Fellowship from the Spanish Ministerio de Educación y Ciencia is also gratefully acknowledged.

#### Appendix A. Evaluation of $Z(l_b; l_a; Y)$ at $u = 0$ for short-ranged forces.

The evaluation of the interfacial properties at the filling boundary  $u = 0$  is based on the knowledge of the partition function (6). In this Appendix we will evaluate explicitly the partition function  $Z(l_b; l_a; Y)$  at the tricritical and critical points for short-ranged forces, and we will discuss some properties of the partition function for arbitrary  $u$ .

Our starting point is the solution of (18), for  $\langle l \rangle = 2$ ,  $V_w(l) = 0$ , so the effective potential is  $V_w(l) = 5l^2$ . This Hamiltonian has  $(1;1)$  deficiency indexes on the  $(0;1)$  interval, so the solution is not unambiguously defined, but instead depends on a parameter  $c$  which defines the short-distance behaviour of the eigenfunctions, i.e.

$$(1) \quad c^{5=6} + \frac{2^{2=3} (1=3)}{(1=3)} l^{1=6} = 0 \quad (A.1)$$

We define the partition function  $Z(l_b; l_a; Y)$  via the spectral expansion:

$$Z(l_b; l_a; Y) = \sum_X (l_b) (l_a) e^{-E_X Y} \quad (A.2)$$

where the summation must be understood as an integral for the continuous part of the spectrum. From (17), this partition function is related to  $Z(l_b; l_a; Y)$  via:

$$Z(l_b; l_a; Y) = \frac{2}{\pi} (l_b l_a)^{1=4} Z(l_b; l_a; Y) \quad (A.3)$$

The continuous part of the spectrum of any self-adjoint extension of our interfacial Hamiltonian corresponds to  $E > 0$ . The corresponding scattering states can be expressed as [37]:

$$E(l) = \frac{p - \frac{h}{c} J_{1=3} \left( \frac{p}{2E} \right) - (2E)^{1=3} J_{1=3} \left( \frac{p}{2E} \right)^{1=3}}{\frac{p^2}{c^2} - \frac{c(2E)^{1=3}}{c(2E)^{1=3} + (2E)^{2=3}} \quad (A.4)}$$

where  $J_s(x)$  is the  $s$ -order Bessel function of first kind.

In addition, for  $c > 0$  there is a bounded eigenstate:

$$0(l) = \frac{3^{3=2} c^3}{\pi} K_{1=3} (c^{3=2} l) \quad (A.5)$$

with associated eigenvalue  $E_0 = \frac{c^2}{4}$ , where  $K_s(x)$  is the  $s$ -order modified Bessel function of second kind. Transforming back to the original variable  $l = (9=8)^{1=3} (2=3)$ , the associated eigenfunction  $0(l)$  is:

$$0(l) / \frac{1}{u} Ai \frac{1}{u} \quad (A.6)$$

where  $A_i(x)$  is the Airy function, and  $u$  is defined:

$$u = \frac{1}{2} \frac{1}{c} = \frac{4}{c} \frac{E_0}{E} \quad (A.7)$$

On the other hand, the longitudinal correlation length along the wedge axis reads  $\gamma = 2=c^3$ . Comparison with the results obtained by the regularization procedures in the text allows us to identify  $c / (u - u_c)$ .

For general  $c$ , we cannot perform the spectral integral. However, for  $c = 0$  ( $u = u_c$ ) and  $c = 1$  ( $u = u_c$ ) we have closed form expressions for  $Z(l_b; l_a; Y)$  [38, 39]:

$$\begin{aligned} Z_{c=0} &= \frac{p}{a-b} \int_0^{\infty} dE e^{-EY} J_{\frac{1}{3}}\left(\frac{p}{2E} a\right) J_{\frac{1}{3}}\left(\frac{p}{2E} b\right) \\ &= \frac{p}{Y} \exp\left(-\frac{b^2 + a^2}{2Y}\right) I_{\frac{1}{3}}\left(\frac{a-b}{Y}\right) \end{aligned} \quad (A.8)$$

$$\begin{aligned} Z_{c=1} &= \frac{p}{a-b} \int_0^{\infty} dE e^{-EY} J_{\frac{1}{3}}\left(\frac{p}{2E} a\right) J_{\frac{1}{3}}\left(\frac{p}{2E} b\right) \\ &= \frac{p}{Y} \exp\left(-\frac{b^2 + a^2}{2Y}\right) I_{\frac{1}{3}}\left(\frac{a-b}{Y}\right) \end{aligned} \quad (A.9)$$

with the scaling property:

$$Z_{c=0, 1} = \frac{1}{Y} U_c \frac{a}{Y}; \frac{b}{Y} \quad (A.10)$$

Substituting into (A.3) we obtain

$$Z_{c=0} = \frac{l_a l_b}{3 u Y} \exp\left(-\frac{(l_a)^3 + (l_b)^3}{9Y}\right) I_{\frac{1}{3}}\left(\frac{2(l_a l_b)^{3/2}}{9Y}\right) \quad (A.11)$$

$$Z_{c=1} = \frac{l_a l_b}{3 u Y} \exp\left(-\frac{(l_a)^3 + (l_b)^3}{9Y}\right) I_{\frac{1}{3}}\left(\frac{2(l_a l_b)^{3/2}}{9Y}\right) \quad (A.12)$$

where  $l = l_u$  and  $Y = \gamma$ . Now the lengthscale  $u$  is arbitrary but  $\gamma = 4 \frac{3}{u} = \frac{3}{u}$ . In both cases we have scaling such that

$$Z_c = Y^{-1/3} U_c \frac{l_a}{Y^{1/3}}; \frac{l_b}{Y^{1/3}} \quad (A.13)$$

for  $c = 0$  and  $1$ . For  $Y \neq 1$ ,  $U_c$  has the following asymptotic behaviour:

$$U_{c=0} \sim \frac{l_a}{Y^{1/3}} \frac{l_b}{Y^{1/3}} \quad (A.14)$$

$$U_{c=1} \sim \frac{l_a}{Y^{1/3}} \frac{l_b}{Y^{1/3}} \quad (A.15)$$

To obtain results for arbitrary  $c$ , we will make use of the Krein formula [40], which relates the Green functions of different self-adjoint extensions of a closed symmetric operator. In our case, the Green function  $Z(l_b; l_a; E)$  is basically the Laplace transform of  $Z(l_b; l_a; Y)$  with respect to  $Y$ :

$$Z(l_b; l_a; E) = \int_0^{\infty} dY \exp(EY) Z(l_b; l_a; Y) \quad (A.16)$$

For  $c = 0$  and  $c = 1$  we have the closed expressions for the Green function [8]:

$$Z_{c=0} = \frac{2}{3} \frac{y l_a l_b}{u} K_{\frac{1}{3}} \frac{2^q}{E(l_b)^3} I_{\frac{1}{3}} \frac{2^q}{E(l_c)^3} \quad (\text{A.17})$$

$$Z_{c=1} = \frac{2}{3} \frac{y l_a l_b}{u} K_{\frac{1}{3}} \frac{2^q}{E(l_b)^3} I_{\frac{1}{3}} \frac{2^q}{E(l_c)^3} \quad (\text{A.18})$$

where  $l_b$  and  $l_c$  are the largest and smallest between  $l_a$  and  $l_b$ , respectively, and  $E = E_y$ .

To continue, we define the lengthscales  $u$  and  $y$  for each  $c$  as:

$$u = \frac{1}{2} \frac{1}{\frac{2^p}{E(l_b)^3}} \quad (\text{A.19})$$

$$y = \frac{2}{\frac{2^q}{E(l_c)^3}} \quad (\text{A.20})$$

Note that  $u$  and  $y$  reduce to the relevant correlation lengthscales for  $c > 0$ . Application of the Kramers formula leads to the following expression for the Green function corresponding to an arbitrary  $c$ :

$$Z_c(l_b; l_a; E) = Z_{-1}(l_b; l_a; E) + g l_a l_b K_{\frac{1}{3}} \frac{2^p}{E(l_a)^3} K_{\frac{1}{3}} \frac{2^q}{E(l_b)^3} \quad (\text{A.21})$$

where  $g = g(E; \dots)$  is obtained by imposing that the short-distance behaviour of  $Z$  is consistent with the boundary condition (A.1). After some algebra, we obtain the following expression:

$$Z_c = \frac{Z_{-1}}{1 - (\frac{E}{E})^{1/3}} - \frac{(\frac{E}{E})^{1/3} Z_0}{1 - (\frac{E}{E})^{1/3}} \quad (\text{A.22})$$

where the negative sign corresponds to  $c > 0$ , and the positive sign to  $c < 0$ . It is worthwhile to note that the dependence on the boundary condition, i.e.  $c$ , has been absorbed into the lengthscales  $u$  and  $y$ . We can formally invert (A.22):

$$Z_c(l_b; l_a; Y) = \frac{1}{2} \frac{Z_{-1}}{i} \int_{-i}^{+i} dE \exp(-EY) Z_c(l_b; l_a; E) \quad (\text{A.23})$$

with  $Y < m \in (0; \sqrt{2})$ . Note that there is a branch point of  $Z_c$  at  $E = 0$ . In addition, there is a single pole for  $E = \sqrt{2}$  for  $c > 0$ . The scaling properties of  $Z_c$  (A.22) lead to the following scaling:

$$Z_c(l_b; l_a; Y) = \frac{1}{u} Z \frac{l_b}{u} \frac{l_b}{u} \frac{Y}{y} \quad (\text{A.24})$$

(A.23) provides a means of obtaining the asymptotic behaviour of  $Z_c$  as  $Y \rightarrow 1$ . For  $c > 0$ , the dominant contribution comes from the pole of  $Z_c$  at  $E = \sqrt{2}$ , so:

$$Z_c(l_b; l_a; Y) \sim \frac{p}{u} \frac{6}{3} \frac{p}{l_a l_b} A(l_a) A(l_b) \exp(Y) \quad (\text{A.25})$$

in complete agreement with our previous analysis. Thus  $u$  and  $y$  are true correlation lengths.

For  $c < 0$ , the branch point of  $Z_c$  at  $E = 0$  controls the large- $Y$  behaviour of  $Z_c$ . We expand  $Z_c$  around  $E = 0$ :

$$\begin{aligned}
 Z_c &= \frac{s}{\frac{1}{\lambda_b}} + \frac{3^{2/3} \frac{1}{3} p \frac{1}{\lambda_a \lambda_b}}{\frac{1}{3} \frac{1}{\lambda_b}} + \dots \\
 &+ (E)^{1/3} \frac{\frac{1}{3} p \frac{1}{\lambda_a \lambda_b}}{3^{2/3} \frac{1}{3}} + \frac{s}{\frac{1}{\lambda_b}} + \frac{3^{2/3} \frac{1}{3} p \frac{1}{\lambda_a \lambda_b}}{\frac{1}{3}} \\
 &+ O(E)^{2/3}
 \end{aligned} \tag{A 26}$$

Thus  $Z_c$  has for large  $Y$  the following asymptotic behaviour:

$$\begin{aligned}
 Z_c &= \frac{\frac{1}{\lambda_a \lambda_b}}{\frac{1}{3} (Y)^{4/3}} + \frac{\frac{1}{3} p \frac{1}{\lambda_a \lambda_b}}{3^{2/3} \frac{1}{3}} + \frac{s}{\frac{1}{\lambda_b}} + \frac{s}{\frac{1}{\lambda_b}} \\
 &+ \frac{3^{2/3} \frac{1}{3} p \frac{1}{\lambda_a \lambda_b}}{\frac{1}{3}} + \dots
 \end{aligned} \tag{A 27}$$

Consequently, we find that for  $\lambda_a, \lambda_b > 1$  but  $p \frac{1}{\lambda_a \lambda_b} = (Y)^{1/3}$  small, the asymptotic behaviour of  $Z_c$  is the same as for the  $c = -1$  case, i.e. critical filling. For the  $c < 0$  case  $u$  and  $y$  are not correlation lengths, but the (microscopic) lengthscales for  $l$  and  $Y$ , respectively, so the critical filling behaviour is observed over larger scales than these.

In order to obtain the asymptotics of the correlation function  $h(\lambda_b; \lambda_a; Y)$  for  $c > 0$ , we also need the next-to-leading order dependence of  $Y$  that emerges from  $Z_c(\lambda_b; \lambda_a; Y)$ . Our approach provides a systematic means of obtaining such correction which can be obtained in a similar manner as before. If we denote by  $Z_c^1$  the leading contribution to  $Z_c$  given by (A 25), the first correction is given by:

$$\begin{aligned}
 Z_c - Z_c^1 &= \frac{\frac{1}{\lambda_a \lambda_b}}{\frac{1}{3} (Y)^{4/3}} + \frac{\frac{1}{3} p \frac{1}{\lambda_a \lambda_b}}{3^{2/3} \frac{1}{3}} + \frac{s}{\frac{1}{\lambda_b}} + \frac{s}{\frac{1}{\lambda_b}} \\
 &+ \frac{3^{2/3} \frac{1}{3} p \frac{1}{\lambda_a \lambda_b}}{\frac{1}{3}} + \dots
 \end{aligned} \tag{A 28}$$

## References

- [1] Gau H, Hergenhahn S, Lenz P and Lipowsky R 1999 *Science* 283 46
- [2] Rascon C and Parry A O 2000 *Nature* 407 986
- [3] Bruschil, Carlin A and Mistura G 2002 *Phys. Rev. Lett.* 89 166101
- [4] Rejmer K, Dietrich S and Napiorkowski M 1999 *Phys. Rev. E* 60 4027
- [5] Parry A O, Rascon C and Wood A J 2000 *Phys. Rev. Lett.* 85 345
- [6] Parry A O, Wood A J and Rascon C 2001 *J. Phys.: Condens. Matter* 13 4591
- [7] Greenall M J, Parry A O and Romero-Enrique J M, 2004 *J. Phys.: Condens. Matter* 16 2515
- [8] Bednorz A and Napiorkowski M 2000 *J. Phys. A: Math. Gen.* 33 L353
- [9] Henderson J R 2004 *J. Chem. Phys.* 120 1535
- [10] Henderson J R 2004 *Phys. Rev. E* 69 061613
- [11] Henderson J R 2005 *Model Sim.* 31 435
- [12] Rascon C and Parry A O 2005 *Phys. Rev. Lett.* 94 096103
- [13] Romero-Enrique J M and Parry A O 2005 *J. Phys.: Condens. Matter* 17 S3487
- [14] Romero-Enrique J M and Parry A O 2005 *Europhys. Lett.* 72 1004
- [15] Bruschil, Carlin A and Mistura G 2001 *J. Chem. Phys.* 115 6200

- [16] Bruschi L, Carlin E and M istura G 2003 *J. Phys.: Condens. Matter* 15 S315
- [17] Bruschi L, Carlin A, Parry A O and M istura G 2003 *Phys. Rev. E* 68 021606
- [18] Milchev A, M uller M , Binder K and Landau D P 2003 *Phys. Rev. Lett.* 90 136101
- [19] Milchev A, M uller M , Binder K and Landau D P 2003 *Phys. Rev. E* 68 031601
- [20] Binder K , M uller M , Milchev A and Landau D P 2005 *Comput. Phys. Comm.* 169 226
- [21] Concus P and Finn R 1969 *Proc. Natl. Acad. Sci. USA* 63 292
- [22] Pomeau Y 1986 *J. Colloid Interface Sci.* 113 5
- [23] Hauge E H 1992 *Phys. Rev. A* 46 4994
- [24] Burkhardt T W 1989 *Phys. Rev. B* 40 6987
- [25] Thomsen J, Enevoll G T and Hemmer P C 1989 *Phys. Rev. B* 39 12788
- [26] Chetouani L, Dekar L and Hammann T F 1995 *Phys. Rev. A* 52 82
- [27] Yu J and Dong S-H 2004 *Phys. Lett. A* 325 194
- [28] Parry A O, Greenall M J and Wood A J 2002 *J. Phys.: Condens. Matter* 14 1169
- [29] Lipowsky R and Nieuwenhuizen T M 1988 *J. Phys. A: Math. Gen.* 21 L89
- [30] Parry A O, Macdonald E D and Rascon C 2001 *J. Phys.: Condens. Matter* 13 383
- [31] Fisher M E 1984 *J. Stat. Phys.* 34 667
- [32] Fisher M E 1986 *J. Chem. Soc. Faraday Trans. 2* 82 1569
- [33] Lebedev N N 1972 *Special Functions and their applications* (New York: Dover Publications Inc.)
- [34] Fyodorov Y V 2005 *Recent Perspectives in Random Matrix Theory and Number Theory*, ed F Mezzadri and N C Snaith (Cambridge: Cambridge University Press)
- [35] Julicher F, Lipowsky R and M uller-Krumbhaar H 1990 *Europhys. Lett.* 11 657
- [36] Spohn H 1991 *Europhys. Lett.* 14 689
- [37] Titchmarsh E C 1969 *Eigenfunction Expansions Associated with Second-Order Differential Equations, Part. I* (Oxford: Clarendon Press)
- [38] Erdelyi A (ed) 1954 *Tables of Integral Transforms, Vol. 1* (New York: McGraw-Hill)
- [39] Gradshteyn I S and Ryzhik I M 1994 *Table of Integrals, Series and Products* (New York: Academic Press)
- [40] Albeverio S, Gesztesy F, Hoegh-Krohn R and Holden H 1988 *Solvable Models in Quantum Mechanics* (New York: Springer)